CERN-TH.5781/90

NUCLEUS-NUCLEUS INTERACTION DYNAMICS AND THE GLAUBER-GRIBOV APPROACH

A. Kaidalov*)
CERN - Geneva

A space-time picture of high-energy hadron-nucleus and nucleus-nucleus interactions is discussed. Predictions of the standard Glauber approach for elastic scattering and multiparticle production in heavy ion collisions are reviewed. Simple expressions for atomic number dependences of inclusive spectra are given. It is pointed out that enhanced diagrams which describe interactions between strings can be important for heavy ion collisions. Prospects for future experiments with very heavy ions and at very high energies are discussed.

---

*) Permanent address: ITEP, B. Cheremushkinskaya ul. 25, 117 259 Moscow, USSR.

CERN-TH.5781/90
June 1990

1. Introduction

Experiments with heavy ion beams at high energies give important information about the properties of strong interactions. A main goal of these studies is to obtain a new state of hadronic matter quark-gluon plasma (QGP), predicted by QCD, and to investigate its properties. However, after many years of theoretical studies it is not yet clear whether QGP can be formed in heavy-ion collisions and whether a thermalized state can be obtained in these processes.

On the other hand, there is a "traditional" approach to nucleus-nucleus interactions based on the Glauber formalism [1,2] of multiple interactions of nucleons. There are many versions of this approach [3-14] (mostly Monte Carlo), which differ in detail but have in common an assumption that different nucleons of nuclei interact independently. A possibility of secondary interactions of produced particles has been taken into account in some of the recent models [10-14]. In general these models give a good quantitative description of experimental data, and allow one to understand global properties of nucleus-nucleus (AB) collisions in terms of nucleon-nucleon interactions. The success of this approach indicates that under present conditions plasma formation is not very important and one should look for some rare processes and subtle correlations in order to find its signals.

In such a situation it is necessary to understand what are the exact (model-independent) predictions of the traditional approach, based on the Glauber-Gribov [1,2] formalism, for nucleus-nucleus interactions. This problem will be discussed in the first part of my talk, together with a short review of the space-time picture of hadron-nucleus and nucleus-nucleus

interactions. The second question, which I will consider is what are possible generalizations of present dynamical models and under what conditions in AB-collisions one can hope to have a thermalized system. Consequences of this general approach, which takes into account interactions between pomerons (or strings), will be given. Prospects for future experiments with very heavy ions (like Pb-Pb collisions) will be discussed and the importance of very high energy nucleus-nucleus collisions (RHIC,LHC) will be emphasized.

2. Space-Time Picture of High Energy Interactions

In this section I want to recall some rather general facts about the space-time picture of high energy interactions [15,16,17], which are valid for hh, hA and AB collisions.

a) Fast-moving hadron or nucleus can be considered as a system of constituents, which is characterized by a wave function, which is a Fock-state vector. For example, a nucleon is a system of quarks, antiquarks and gluons

$$|N\rangle = \left| \begin{array}{l} 3q \\ 3q + kg \\ 3q + kg + mq\bar{q} \end{array} \right\rangle$$

b) A content of the state *i.e.*probabilities of different configurations, is Lorentz-frame dependent. The most adequate frame for high energy scattering processes is the infinite momentum frame (IMF). Note that a space-time picture of the interaction is in general different for different Lorentz frames.

c) Partonic configurations of a fast-moving hadron have long lifetimes $\tau \sim \frac{E}{\mu^2}$.

d) Fast parton components of wave functions are Lorentz-contracted, $-\ell \sim \frac{1}{p} \sim \frac{1}{p_0 x}$, while soft ones ($x \simeq 0, p \sim \mu$) are not. So hadrons, as well as nuclei at any energy have finite longitudinal size.

e) In the rest-frame of a target interaction is initiated by soft partons of a projectile.

Let us consider hadron-nucleus collisions from this point of view. It has already been understood long ago (see, e.g., Ref. 2) that a space-time picture of an interaction is completely different at comparatively low energies $E < E_0 = \mu^2 R_A$, where μ is some characteristic hadronic scale and R_A is the radius of nuclei, and at high energies $E > E_0$. At low energies $E < E_0$, the Glauber approximation in a field theory as well as for potential scattering corresponds to successive rescatterings of the initial particle on nucleons of nuclei (Fig. 1). However at energies $E > E_0$ these "planar" diagrams decrease as $\frac{1}{E}$ [18].

This is connected to the fact that formation time for a particle h in the intermediate state (Fig. 1b) $\tau \sim \frac{E}{\mu^2}$ in this energy range is larger than the dimension of a nucleus. On

the other hand, the non-planar diagrams of Fig. 2, which are small at $E < E_0$, start to be important at high energies $E > E_0$.

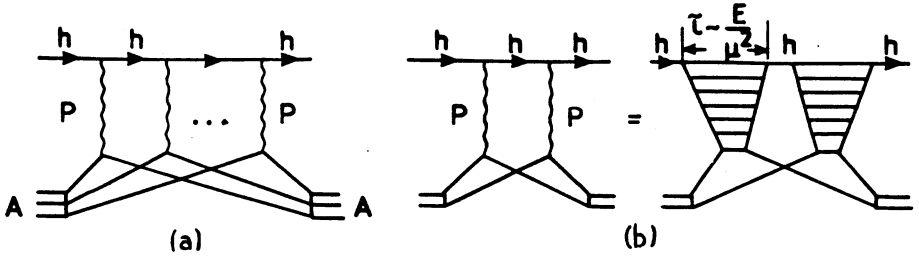

Fig. 1: a) Rescatterings of the initial hadron on nucleons of nuclei; b) Space-time structure of double rescattering.

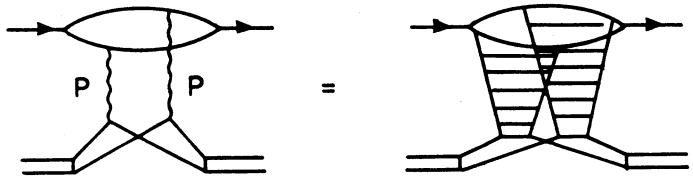

Fig. 2: Non-planar diagram for double rescattering.

These diagrams, first considered by Mandelstam [18], do not decrease with energy and correspond to simultaneous interactions at the same longitudinal distances of the partonic fluctuation of the initial hadron "prepared" before a collision with a nucleus. Nevertheless, the final formula for a sum of all diagrams for the elastic hA-amplitude is close to the Glauber expression, differing by only the contribution of inelastic diffractive scattering (see Fig. 3, where crosses on the lines indicate that the corresponding particles are on mass shell).

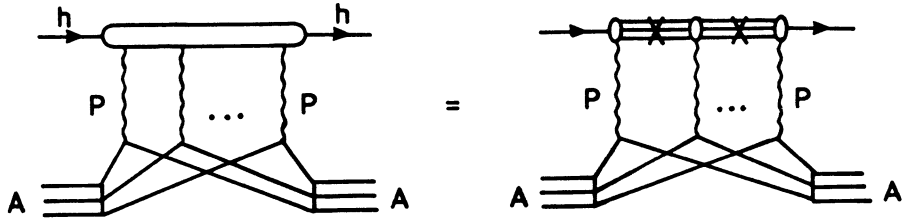

Fig. 3: Gribov's representation of multiple rescattering diagrams.

This has been shown by Gribov [2] with the help of a general approach based on analyticity and unitarity. Possible contributions to discontinuity of the Pomeron (**P**)-particle scattering amplitude are shown in Fig. 4. The first contribution corresponds to elastic rescatterings and leads to the Glauber formula, while other contributions corespond to inelastic diffractive rescatterings and are relatively small ($15 \div 20\%$ of the elastic one). The last term in this fugire corresponds to a contribution of many particle states connected to a large mass diffraction, which is described by a triple Pomeron interaction. Thus a total contribution of rescattering terms f_R to elastic hA-maplitudes have a smooth dependence on energy at $E \sim E_0$ (see Fig. 5) and are close to the Glauber theory, though a space-time picture, as was emphasized above, does not correspond to successive rescatterings of an initial hadron in a nucleus.

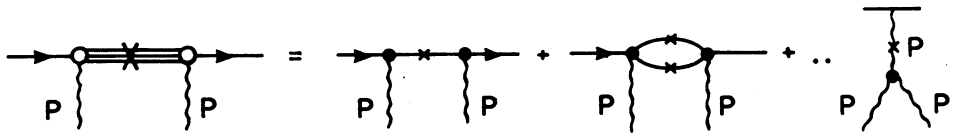

Fig. 4: Contributions of different intermediate states to a discontinuity of the Pomeron-particle scattering amplitude.

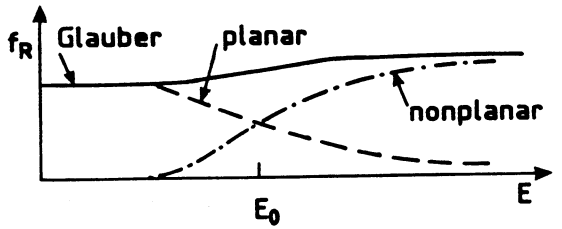

Fig. 5: Energy behaviour of the rescattering amplitude f_R.

Let us consider now a fast-moving nucleus. Its longitudinal size R_L^A is Lorentz-contracted in laboratory frame, but of course it cannot be smaller than the longitudinal size of a nucleon R_L^N which is $\sim \frac{1}{\mu}$. So at any energy $R_L^A \gtrsim R_L^N \sim \frac{1}{\mu}$ and soft partons of different nucleons with $x = \frac{p}{p_0^N} < x_{crit} = \frac{1}{mR_A}$ overlap. Interaction of these soft partons (Fig. 6) corresponds to a definite discontinuity of "enhanced" diagrams, shown in Fig. 6, which usually leads to screening effects. The diagrams of Fig. 6 correspond in particular to a universal distribution of partons (and final hadrons) for hA and hh-interactions for $y - y_A > \ell n \frac{1}{x_{crit}} = \ell n(mR_A)$. This is the picture proposed originally by Kancheli [19], which can be realized if interaction between Pomerons is very strong. However, many-Pomeron couplings g_{mn} are known to be small (see, e.g., [20]). In the 1/N-expansion of QCD ($N = N_c = 3 \approx N_f$), $g_{mn} \sim (\frac{1}{N})^{m+n-2}$. Triple-Pomeron and four-Pomeron couplings can be estimated from experiments on high

mass diffraction dissociation and double-Pomeron exchange (Fig. 7) [20]. If follows from these studies that relative probabilities of 3P-type interactions (7a) (per unit of rapidity) are $w_{3P} \sim \frac{1}{20}$ and of 4P-type interactions (7b) are $\lesssim 10^{-2}$. Thus at energies $S \sim 10^2 - 10^3\ GeV^2$ these interactions are not important in hadronic collisions. However, these probabilities increase for hA-collisions ($\sim A^{1/3}$) and especially for AB-collisions [$\sim (A^{1/3} + B^{1/3})$ for 3P-type and $A^{1/3}B^{1/3}$ for 4P-type]. It is important to understand the role of enhanced diagrams, because they correspond to interactions between strings which are formed in high energy collisions (see below) and in AB-collisions they can lead to thermalization of a system.

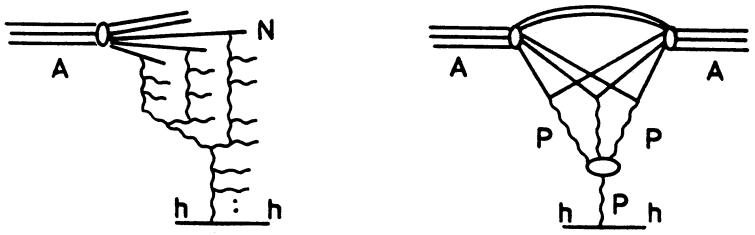

Fig. 6: Interaction of partons and the corresponding enhanced diagram.

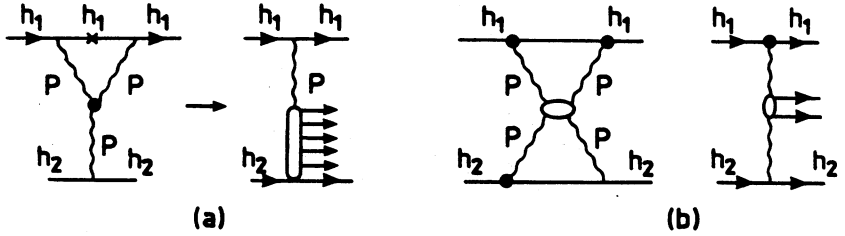

Fig. 7: Triple-Pomeron-(a) and four-Pomeron-(b) interactions and their diffractive cuttings.

In order to reveal experimentally the effects of the diagrams with interaction between Pomerons it is necessary to understand what are the predictions of the approach, based on the Glauber-type non-enhanced diagrams. In the next section we will discuss these predictions.

3. Elastic Scattering and Total Cross-Section for AB Collisions. Loop diagrams

Here we will use the Glauber approach [1] for amplitudes of elastic AB-scattering and $\sigma_{AB}^{(tot)}$. In the case of a hadronic interaction with large nucleus, a very well-known expression for $\sigma_{hA}^{(tot)}$ is

$$\sigma_{hA}^{(tot)} = 2\int d^2b \left[1 - exp\left(-\frac{\sigma_{hN}^{(tot)}}{2} \cdot n_A(\vec{b})\right)\right] \tag{1}$$

where $\vec{b}$ is an impact parameter and $n_A(\vec{b}) = \int dz \rho_A(z, \vec{b})$ is a two-dimensional distribution of nucleons in a nucleus A. Equation (1) has a simple geometrical interpretation (optical approximation). A natural extension of Eq. (1) to the case of nucleus-nucleus scattering has been proposed in Refs. [21,22]

$$\sigma_{AB}^{(tot)} = 2\int d^2b \left[1 - exp\left(-\frac{\sigma_{NN}^{(tot)}}{2}\int d^2a\ n_A(\vec{a}) n_B(\vec{b} - \vec{a})\right)\right] \tag{2}$$

However, it was realized that this formula can be obtained from a very limited class of diagrams shown in Fig. 8a and there is no reason to neglect other types of diagrams shown in Fig. 8.

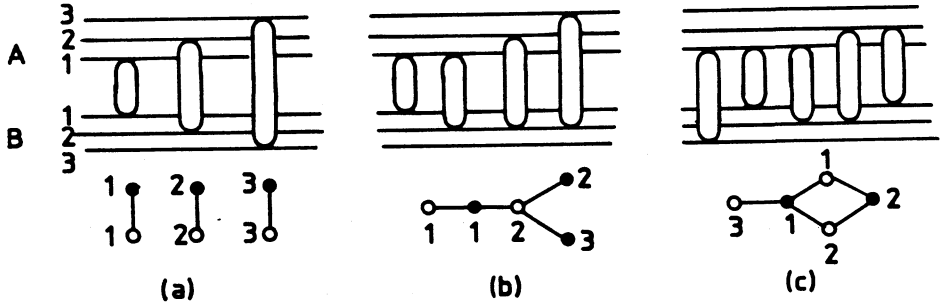

Fig. 8: Different types of diagrams for nucleus-nucleus interactions.

The problem of summation of all tree graphs Fig. 8b and Fig. 9 has been studied in Refs. [23,24], where the diagrams with loops of the type shown in Fig. 8c have been neglected. This was motivated by the fact that loop graphs contain a parameter $\sigma_{\frac{NN}{\sigma_{NN}^{(tot)}}}^{(el)} \approx \frac{1}{4}$.

In our paper [25] a solution of the problem of summation of all diagrams including the ones with loops (Fig. 10) has been obtained. It was shown that the sum of all tree diagrams leads to the optical approximation formula (2). It has also been shown that this is only a first term of the expansion in nuclear densities and the value of the expansion parameter for loop diagrams is not small, so they should be taken into account in any realistic calculation

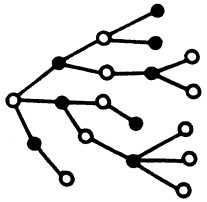

Fig. 9: Tree diagrams.

of nucleus-nucleus collisions. For $\sigma_{AB}^{(tot)}$, the influence of loop diagrams is very small, because already in the tree approximation a profile function in b-space is very close to a black disk limit for all values of b, except the edge region, where overlap of nuclear densities is small. However, loop diagrams can lead to modification of the optical approximation prediction for inelastic processes.

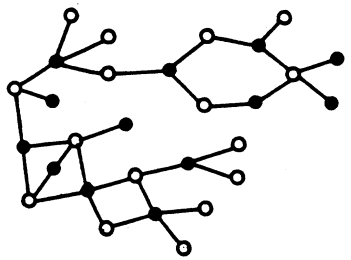

Fig. 10: Diagrams of general type involving loops.

4. Multiparticle Production in Nucleus-nucleus Collisions

In this section, the prediction of the Glauber-Gribov approach for multiparticle production processes in AB-collisions will be considered with special emphasis on the results, which are model independent and can be used for crucial tests of this approach. A role of loop-diagrams will be discussed [26].

The Abramovsky-Gribov-Kancheli cutting ruels (AGK rules) [27] give a possibility to calculate different characteristics of inelastic processes. According to these rules, contributions of different intermediate states to the total cross-section of high energy AB interactions can be determined if the total cross-section $\sigma_{AB}^{(tot)}(b)$ in impact parameter space ($\sigma_{AB}^{(tot)} \equiv \int d^2b\sigma_{AB}^{(tot)}(b)$) is known as a function of $\sigma_{NN}^{(tot)}$. Below we give some consequences of this approach (a simple derivation of them can be found in Ref. [26]).

Let us introduce a function $T_{AB}(b,x) = \sigma_{AB}^{(tot)}(b,x)$ where $x = -\frac{\sigma_{NN}^{(tot)}}{2}$. Then cross-sections of many processes can be determined in terms of this "master function" T_{AB}.

a) Self-Absorption theorem

Consider the cross-section for some selected process (e.g., events with particle production or events with at least one strange particle, or lepton pair, etc.). This cross-section σ_{AB}^{c} is equal to a function $T_{AB}(b,-\sigma_{NN}^{c})$, where σ_{NN}^{c} is the cross-section of the selected process in NN-interactions. For a particular case of particule production cross-section in AB-collisions we have a result

$$\sigma_{AB}^{prod} = T_{AB}(-\sigma_{NN}^{in}) \tag{3}$$

which is well known in the optical approximation (2), but is valid for a sum of arbitrary diagrams. The self-absorption theorem has been formulated for hadron-nucleus collisions in Ref. [28] and was discussed for nucleus-nucleus collisions in Ref. [29]. This result implies that cross-sections of rare processes with $\sigma_{NN}^{c} \ll \sigma_{NN}^{(tot)}$ (e.g., J/ψ-production or Drell-Yan process) are practically not absorbed and $\sigma_{AB}^{c} \simeq AB\sigma_{NN}^{c}$. Let us mention that the contribution of loop diagrams to $T_{AB} \sim x^{4+n}(n \geq 0)$ as $x \to 0$ (the simplest loop contains an interaction of four nucleons) and it strongly depends on σ_{NN}^{c}. Thus varying σ_{NN}^{c} (choosing different selected processes), it is possible to study experimentally the role of loop diagrams.

b) Distribution of the number of inelastic interactions

Consider a distribution of the number of inelastic NN-interactions $\sigma_{AB,K}$. The corresponding generating function $G_{AB}^{prod}(\beta)$

$$G_{AB}^{prod}(\beta) = \sum_{k=1}^{\infty} \sigma_{AB,K}\beta^K \tag{4}$$

is expressed in terms of the function T_{AB} as follows

$$G_{AB}^{prod}(\beta) = T_{AB}(-\sigma_{NN}^{in}) - T_{AB}((\beta-1)\sigma_{NN}^{in}) \tag{5}$$

In the tree approximation

$$G_{(tree)}^{prod}(\beta) = exp[(\beta-1)\sigma_{NN}^{in} n_A \otimes n_B] - exp[-\sigma_{NN}^{in} n_A \otimes n_B] \tag{6}$$

where $n_A \otimes n_B$ denotes a convolution of nucleon distributions in nuclei A and B, as in Eq. (2). Thus, for fixed values of b, cross-sections $\sigma_{AB,K}$ are given by a Poisson distribution

$$\sigma_{AB,K}^{(tree)} = \frac{(\sigma_{NN}^{in} n_A \otimes n_B)^K}{K!} \quad exp(-\sigma_{NN}^{in} n_A \otimes n_B) \tag{7}$$

It follows from Eq. (5) and a structure of amplitude $T_{AB}(x)$ that the first three momenta of the distribution on K do not include loop contributions and coincide with the tree ap-

proximation result. For example, for a first momentum we have

$$\sigma_{AB}^{(prod)}(b)\langle K\rangle_{AB} = (n_A \otimes n_B)\sigma_{NN}^{in} \tag{8}$$

and after integration over b*

$$\langle K\rangle_{AB} = \frac{AB\sigma_{NN}^{in}}{\sigma_{AB}^{prod}} \tag{9}$$

c) Transverse energy

The mean transverse energy in AB-collisions will be given by the product of a mean transverse enrgy in NN-collisions $\langle E_t\rangle_{NN}$ with $\langle K\rangle_{AB}$

$$\langle E_t\rangle_{AB} = \frac{AB\sigma_{NN}^{in}}{\sigma_{AB}^{prod}}\langle E_t\rangle_{NN} \tag{10}$$

Taking into account that $\sigma_{AB}^{prod} \sim (A^{1/3} + B^{1/3})^2$ for heavy nuclei we can conclude that the quantity $\rho_{AB} = \frac{(A^{1/3}+B^{1/3})^2}{AB}\langle E_t\rangle_{AB}$ should not depend on A and B. This agrees with existing data at high energies. A distribution of transverse energy is mainly determined by the distribution on K and thus the first three momenta do not depend on the loop contributions. However, higher momenta involve loop graphs. This in particular means that the large E_t tail of the distribution, which is potentially important for a search of QGP, can be sensitive to loop corrections, which are difficult to control.

d) Inclusive spectra

An important consequence of AGK rules is a theorem of the cancellation of multiple-interaction contributions to inclusive processes [27]. So only the simplest diagram of Fig. 11 contributes, and at high energies the inclusive cross-section $f^c(x_F, p_\perp^2) \approx E \times d^3\sigma^c/d^3p$ for production of the hadron c is equal to

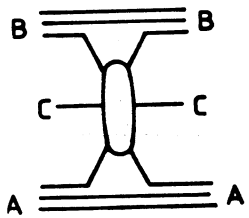

Fig. 11: Diagrams for inclusive cross-sections in the Glauber model.

⋆ The normalization condition is $\int n_{A(B)}(b)d^2b = A$.

$$f_{AB}^c(x_F, p_\perp^2) = ABf_{NN}^c(x_f, p_\perp^2) \tag{11}$$

This formula is valid in the central region ($x_F \ll 1$). The loop graphs do not contribute to the inclusive spectra in the central region. It is easy to see, using AGK rules, that the loop graphs give contributions only starting from the four-particle inclusive cross-section.

If an interaction between Pomerons is essential, then the dependence on A, B given by Eq. (11) is violated. An extra screening due to these interactions (Fig. 12) will lead (for $x_F \ll 1, s \gg m^2, A^{1/3}, B^{1/3} \gg 1$) to

$$f_{AB}^c \sim A^{2/3}B^{2/3} \tag{12}$$

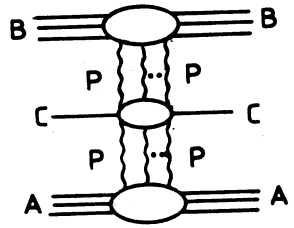

Fig. 12: Diagrams for inclusive cross-section taking into account Pomeron interactions.

Thus experimental measurement of A,B-dependence of inclusive spectra in the central region is important for a crucial test of the Glauber approximation. In the fragmentation region ($x_F \sim 1$) the AGK-cutting rules are violated due to energy-momentum conservation effects [30]. The fact that only those nucleons, which have a small number of inelastic interactions can contribute to the hard part of inclusive spectra, strongly influences A, B dependence of inclusive cross-sections in fragmentation regions. For parametrization of A-dependence of inclusive spectra in hA-interactions $f_{hA}(x_F) \sim A^{\alpha(x_F)}$ the function $\alpha(x_f)$ decreases from 1 at $x_F \simeq 0$ to $0.4 \div 0.5$ as $x_f \to 1$ Fig. 13* (for more details on this subject, see talk of A. Capella at this conference [31]).

It can be shown [26] that in AB collisions the contribution of loop graphs to inclusive spectra cancels even with energy-momentum conservation effects taken into account and

⋆ The function $\alpha(x_F)$ depends on $p_\perp, S$ and a type of particle c. At high energy and small $p_\perp$ $\alpha(x_F)$ is nearly universal for all types of light hadrons.

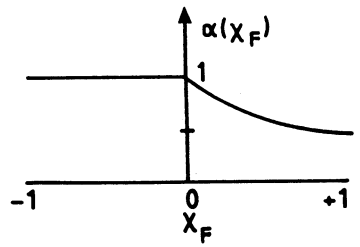

Fig. 13: Function $\alpha(x_F)$ at high energies in the Glauber model.

A,B-dependence of f^c_{AB} is completely determined by the same function $\alpha(x)$ as for hadron-nucleus interactions

$$f^c_{AB}(x_F,p_\perp) \sim A^{\alpha_c(x_F,p_\perp)} B^{\alpha_c(-x_F,p_\perp)} \tag{13}$$

This in particular implies that at energies high enough

$$f^c_{AB}(x_F,p_\perp) = \begin{cases} A f^c_{NB}(x_F,p_\perp) & \text{in A-fragmentation region} \\ B f^c_{NA}(x_F,p_\perp) & \text{in B-fragmentation region} \end{cases} \tag{14}$$

Deviations from these relations decrease with energy as $1\sqrt{s}$ and are already small at present energies $\sqrt{s} \sim 10\ GeV$. So it would be interesting to make a careful comparison of relations (13) and (14) with existing experimental data on hA and AB-collisions in order to find out non-Glauber type contributions.

5. Enhanced diagrams - interactions between strings

In this section I shall discuss in more detail the role of enhanced diagrams, which are connected to interactions between Pomerons, in nucleus-nucleus interactions, and their relation to the models of multiparticle production, based on strings. These models (DTU [32], QGSM [33]) are based on the 1/N-expansion in QCD [34,35] and on the string picture of hadrons in the confinement region. In this approach cylinder-type diagrams, shown in Fig. 14a, correspond to Pomeron exchange and its cutting leads to a multiparticle state which is due to production and subsequent decay of two strings (two chains of hadrons - Fig. 14b). The Glauber-type rescatterings of the initial hadron on different nucleons of nuclei correspond to multicylinder diagrams. Some of the inelastic cuttings of these diagrams lead to the creation of many chains of hadrons (creation and decay of many strings) - Fig. 15. The mean number of chains produced in hA collisions for a given impact parameter is larger than in the NN-case by a factor $\sim A^{1/3}$. In the NN-case, the mean number of chains increases with energy as s^Δ (where $\Delta = \alpha_P(0) - 1 \approx 0.12$), so hadron-nucleus and nucleus-nucleus interactions reveal multiquark configurations in colliding hadrons (nuclei) and in this sense resemble hN interactions at much higher energies.

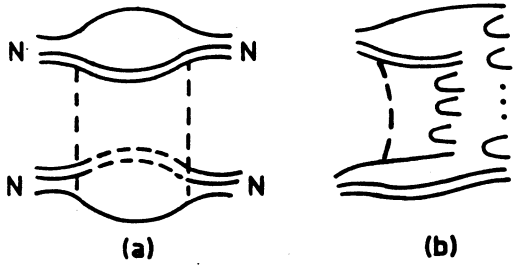

Fig. 14: Cylinder-type diagram (a) and its inelastic cutting (b).

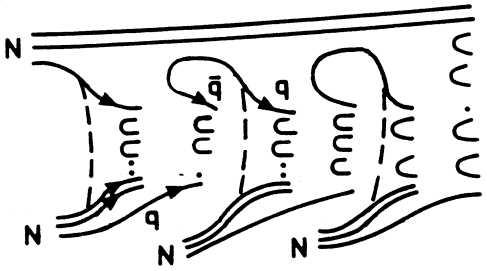

Fig. 15: Diagram for inelastic interaction with several nucleons of nuclei.

In DTU the diagrams are classified according to their topology. So all the secondary interactions, which do not change the topology of a diagram are already included in the diagrams of the type shown in Figs. 14, 15. New topological structures correspond to interactions between strings (Pomerons). For example, the diagram shown in Fig. 7b with a four-Pomeron interaction corrsponds in DTU to the diagram of Fig. 16a, with one extra "handle" which is $\simeq 1/N^2$. One of its possible inelastic cuttings is shown in Fig. 16b and corresponds to interactions between particles produced in different nucleon-nucleon collisions. Relative coefficients for different cuttings are given by AGK cutting rules. Thus, if we know the contribution of diffractive (double-Pomeron) cutting of the diagram, shown in Fig. 7b, we can calculate all other inelastic cuttings.

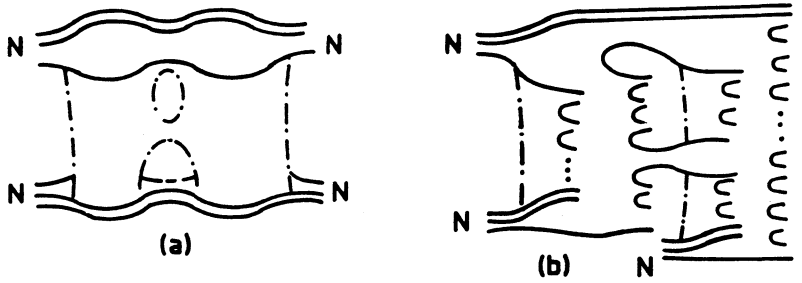

Fig. 16: Example of enhanced diagram,(a) and one of its inelastic cuttings (b).

A formalism, based on a study of cutting rules for Feynman diagrams gives a possibility to discuss properties of secondary rescatterings of produced particles (or partons) in nuclei. Consider, for example, the problem of a "cascade" in a nucleus. It is usually assumed, in calculations, which take into account interactions of produced particles with nucleons of nuclei (Fig. 17) that for particles with momentum k, there is a "formation time" [36,37] $\tau \sim k/\mu^2$. so only particles with $\tau < R_A$ or $k < k_0 = \mu^2 R_A$ can effectively reinteract in a nucleus. It was also claimed in Ref. [38] that the probability of cascading in this region is not connected to the triple-Pomeron vertex g_{PPP}. However, a careful analysis [39] of cutting rules for both planar (Fig. 18a) and non-planar (Fig. 18b) diagrams has shown that:

a) Particles with all k can interact.

b) The probability of rescatterings for particles with $x_F \ll 1$ is proportional to g_{PPP}.

c) Inclusive spectra are enhanced in the region $k < k_0$, as in cascade models.

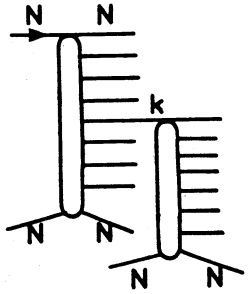

Fig. 17: Inelastic interaction of a produced particle with a nucleon.

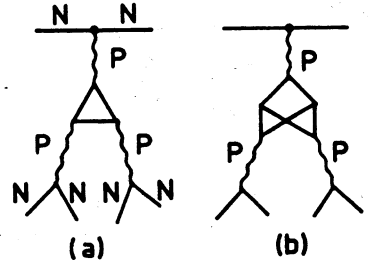

Fig. 18: Triple-pomeron interaction diagrams with planar - (a) and non-planar (b) structure of the vertex

Two different physical pictures of interaction take place for $k < k_0$ and $k > k_0$. The situation is analogous to the one we have discussed in Section 2 for elastic scattering - in the "formation zone" $k < k_0$ one can speak of successive interactions of produced particles with nucleons of nuclei; at larger momenta this is impossible due to formation time effects. However, in this region $k > k_0$ there is a "simultaneous" interaction of soft partons (or

particles), which are in the initial hadronic fluctuation and have been "prepared" before collision with a nucleus. The contribution to the cross-section of configurations, where both nucleons interact inelastically (Fig. 17), varies smoothly in the region $k \sim k_0$. On the other hand it has been found in Ref. [39] that absorption corrections have sharp variations in the region $k \sim k_0$. If we denote by θ a rapidity corresponding to a triple-Pomeron vertex ($\theta \approx \ell n \frac{k}{\mu}$) in Fig. 18 and $\theta_0 = \ell n \frac{k_0}{\mu} = \ell n \mu R_A$, then it turns out that the diagrams of Fig. 18 give a non-vanishing contribution to the total cross-section for $\theta > \theta_0$, while this contribution is zero for $\theta < \theta_0$. For the contribution to the inclusive spectra $f(y)$ (with $y < \theta$) the situation is the opposite - it is zero for $\theta > \theta_0$ and it is different from zero for $\theta < \theta_0$ in the cascade region. So there is an extra positive contribution from enhanced diagrams in this region. Thus, with the help of the diagrammatic technique, which takes into account all absorption effects, it was possible to prove the usual assumptions of the cascade model in the region $k < k_0$. Secondary interactions do not change the cross-section, but they increase the number of produced particles and change their spectra. An essential difference of this technique with a naive cascade model is that in Reggeon theory also fast particles (with $k > k_0$) interact and produce additional particles. This is compensated in inclusive spectra by additional absorption, but many-particle inclusive cross-sections are influenced by these contributions. Note that in the region $y > \theta$ the enhanced diagrams of Fig. 18 lead to extra absorption for inclusive spectra.

Inclusion of enhanced diagrams with interaction of strings leads to many qualitative effects in hA and AB-interactions

a) Inclusive spectra

The prediction of the Glauber model for very high energies when the total rapidity interval $\ell n \frac{s}{m^2} \gg \theta_0$. The prediction of the Glauber model (A^1-dependence of f_{hA} in the central region and the target A-fragmentation region - full line in Fig. 19) is modified by enhanced diagrams, as shown schematically by the dashed line of Fig. 19. There is a decrease compared to the Glauber model in the central region and an increase in the nucleus fragmentation region. A-dependences for very strong interactions of Pomerons are indicated. Present data on hA-interactions do not cover a large enough rapidity interval to draw a definite conclusion, but it seems that they are closer to the Glauber model prediction, indicating that interactions between strings are not very important (see, [31]).

For AB-collisions a situation is illustrated in Fig. 20. At present energies the total rapidity interval $\ell n \frac{s}{m^2} \lesssim 6$ is not much larger than $\theta_0^A + \theta_0^B (\theta_0 \approx \ell n m R_A \sim 3)$, and it is difficult to study a central region. Higher energies $\sqrt{s} \gtrsim 10^2\ GeV$ are needed in order to study A,B-dependence separately in the central and fragmentation regions and to investigate in detail string interactions.

b) Correlations

Inclusion of enhanced diagrams leads to a strong modification of A,B-dependences of

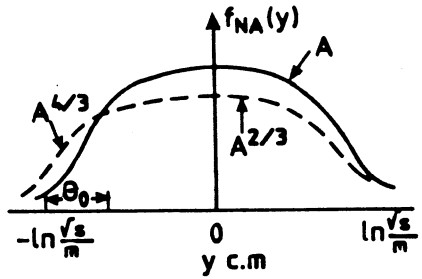

Fig. 19: A-dependence of inclusive spectra in hA collisions at very high energies. Full line - Glauber model; dashed one - for strong interaction between Pomerons.

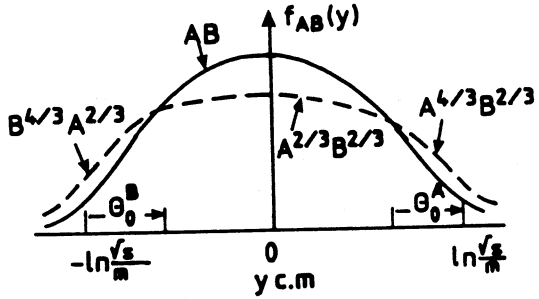

Fig. 20: Same as in Fig. 18 for AB-collisions.

many particle inclusive cross-sections and correlation functions. It is interesting to note that the identical particle correlations are also connected to the enhanced diagrams as is indicated in Fig. 21.

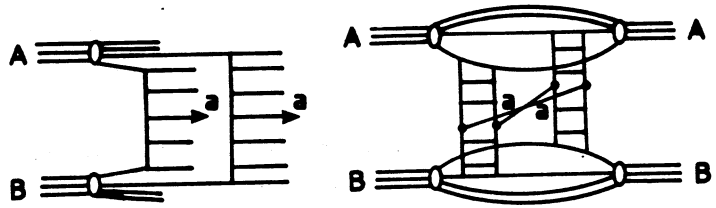

Fig. 21: Simplest diagrams corresponding to correlations between identical particles.

c) Direct photons

In the independent nucleon interaction models, a number of direct photon n^γ is proportional to a number of charged particles n_{ch}. Taking into account interactions between

Pomerons, this dependence changes to $n_\gamma \sim n_{ch}^2$ [40]. So an observation of such a dependence is not a signal of QGP, but rather indicates strong secondary interactions.

d) J/ψ-suppression, ϕ-enhancement

An extra A,B-dependence (or E_T-dependence) in AB-collisions, compared to hA-collisions can be connected to the influence of enhanced diagrams. The size of the effects depends on the values of many Pomeron couplings with a given particle c, shown for inclusive cross-sections in Fig. 22. A particular example of these enhanced diagrams (fan type diagrams due to triple-Pomeron interaction - Fig. 22) has been considered in [41] for J/ψ-production and leads to a reasonable description of J/ψ-suppression in nucleus-nucleus collisions. Relative enhancement of ϕ-mesons, observed recently by the NA38 collaboration [42], can also be accommodated in the same scheme, if we take into account that ϕ can be effectively produced by secondary kaons from different nucleon-nucleon collisions, (there is no such effect for J/ψ). It should be also taken into account that ϕ are measured at rather large p_t, where effects of initial state rescattering can be important.

Thus interactions between strings lead to many effects which have been originally proposed as signals for QGP and it will be difficult to find experimentally clear evidence for QGP.

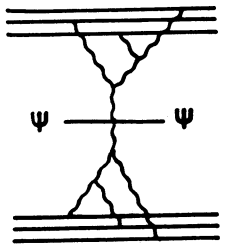

Fig. 22: Enhanced diagrams of "fan"-type for inclusive J/ψ-production.

6. Extrapolations to higher energies and very heavy ions

Interactions between strings are important for understanding a problem of thermalization in heavy ion collisions. In order to obtain "collectivization" of partons belonging to different nucleons, and to produce a system in equilibrium, it is necessary to have a mean number of interactions between strings $\bar{n}_{AB} \gg 1$. Values of $\bar{n}_{AB}(s)$ can be estimated as follows:

$$\bar{n}_{AB}(s) \approx \bar{n}_{NN}(s) A^{1/3} B^{1/3} w_{4P} \tag{15}$$

where $\bar{n}_{NN}(s)$ is a mean number of strings in NN-collisions, $A^{1/3}B^{1/3}$ is a mean number of interacting nucleons in a tube of nucleon size (this is for average collisions, for central

collisions this number can be several times larger), and w_{4P} is a probability of string (4-Pomeron) interaction. For 3P-interaction (coalescence and splitting of strings) the factor $A^{1/3}B^{1/3}$ should be changed to $(A^{1/3}+B^{1/3})$. The quantity $\bar{n}_{NN}(s)$ in the supercritical Pomeron theory increases as $(\frac{s}{s_0})^{\Delta}$ with $\Delta \approx 0.12$ [33] and $\bar{n}_{NN}(s) \approx 1$ for $\sqrt{s} \approx 10\ GeV$. Using for an estimate $W_{3P} \simeq 0.05, W_{4P} \simeq 0.01$, we obtain the values of $n_{AB}(s)$ given in Table 1 for $\sqrt{s} = 20\ GeV$ and LHC energies.

	3P-interaction		4P-interaction	
	$\sqrt{s}$ = 20 GeV	$\sqrt{s}$ = 7•10^3 GeV	$\sqrt{s}$ = 20 GeV	$\sqrt{s}$ = 7•10^3 GeV
pPb	0.35	1.4	0.07	0.28
OPb	0.5	2.0	0.15	0.6
PbPb	0.7	2.8	0.36	1.44

Table 1

Values of $\bar{n}_{AB}$ for 3P and 4P-interactions at different energies.

Note that these numbers correspond to $\bar{n}_{AB}(s)$ per unit of rapidity in the central region. Though these numbers are subject to rather large uncertainties due to our poor knowledge of W_i we can conclude that interaction of strings is not large at $\sqrt{s} = 20\ GeV$, though for Pb-Pb central collisions it can reach a critical value. Some predictions for multiplicity and transverse energy distributions for very heavy ion collisions (Au-Au) at $\sqrt{s} = 20\ GeV$ [13] are shown in Fig. 23. Energy density, estimated with the help of the Bjorken formula [43], is rather large $\epsilon \sim 5\ GeV/fm^3$, but it is achieved for a very small period of time [13]. This also indicates that thermal equilibrium is not yet achieved at these energies even for very heavy ions. However, all the phenomena due to string interactions will be substantially increased for very heavy ion collisions.

At LHC energies, interaction of strings is much more important (see Table 1). So at energies of RHIC and LHC it is not only possible to study separately the central and fragmentation regions, but one can hope to have a quark-gluon state close to equilibrium in heavy-ion collisions. It is not clear, however, that this state will be QGP. Interaction of pomerons leads in general to screening of partons, belonging to different nucleons in a central region and it is possible that some universal system will be created in the central region in hh, hA and AB collisions.

Let us summarize our main conclusions.

1) Models based on independent interactions of nucleons describe the main features of the present data on nucleus-nucleus collssions.

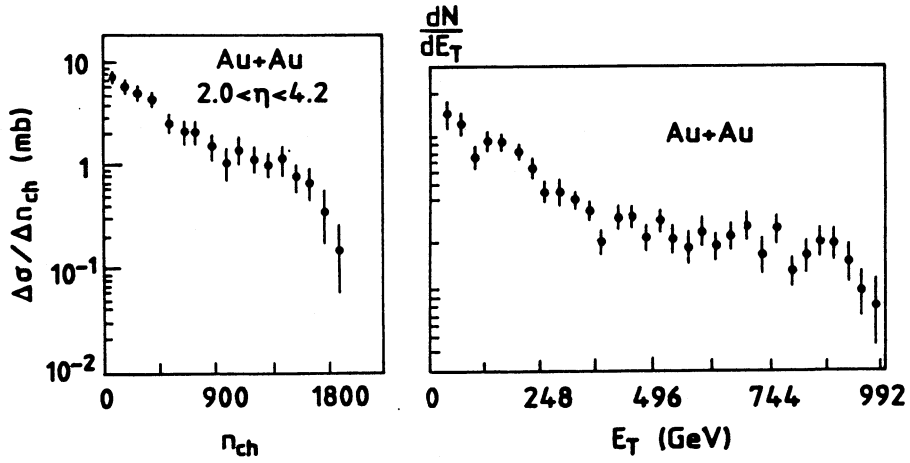

Fig. 23: Predictions for multiplicity (a) and transverse energy (b) distributions in Au-Au interactions at energy 200 GeV/nucleon [13].

2) Atomic number dependences of inclusive cross-sections can be used for crucial tests of the Glauber model.

3) Interactions between strings are determined by many-Pomeron couplings and are small. These interactions are enhanced in AB collisions and can imitate QGP effects.

4) Extrapolation to heavier ion beams (Pb) shows that new phenomena can reach a critical level.

5) Increase of initial energy to RHIC and LHC energy regions is very important for the understanding of dynamics of nuclear collisions and the problem of QGP formation.

ACKNOWLEDGEMENTS

I am indebted to K.G. Boreskov, A. Capella, J. Ranft and J. Tran Thanh Van for useful discussions and acknowledge the warm hospitality of the theory groups of Orsay and CERN where this work was completed.

REFERENCES

[1] R.J. Glauber, Lect. in Theor. Phys., Ed. W.E. Britten, Interscience Publ., N.Y., 1959, Vol. 1 p. 315;
A.G. Sitenko, *Ukr. Phys. Journ.* **4** (1959) 152.

[2] V.N. Gribov, *JETP* **56** (1959) 982; **57** (1969) 1306.

[3] A. Capella, J. Kwiecinski and J. Tran Thanh Van, *Phys. Lett.* **108B** (1982) 347;
A. Capella, C. Pajares and A.V. Ramallo, *Nucl. Phys.* **241** (1984) 75;
A. Capella et al., *Zeit. Phys.* **C27** (1985) 413.

[4] J. Ranft and S. Ritter, *Zeit. Phys.* **C27** (1985) 413.

[5] A.M. Zadorozhnyi, V.V. Uzhinskii and S.Yu. Shmakov, JINR report P2-86-361, Dubna (1986).

[6] N. Amelin, JINR Report P2-86-802, Dubna (1986).

[7] M. Gyulassy, CERN preprint TH.4794/87 (1987).

[8] B. Anderson, G. Gustafson and B. Nielsson-Almqvist, *Nucl. Phys.* **B281** (1987) 289.

[9] T.P. Pansart, *Nucl. Phys.* **A461** (1987) 521.

[10] J. Ranft, *Phys. Rev.* **D37** (1988) 1842.

[11] K. Werner, *Phys. Lett.* **B208** (1988) 520; **B219** (1988) 111; *Phys. Rev.* **D39** (1989) 780;
K. Werner and P. Koch, CERN preprint TH.5607/89 (1989).

[12] A. Shor and R. Longacre, *Phys. Lett.* **B218** (1989) 100.

[13] N.S. Amelin, K.K. Gudima and V.D. Toneev, Proc. of the XI International Seminar on High Energy Physics Problems, Dubna, 1988, D1, 2-88-652, vol. 1, 389; preprint GSI-89-52; Yad. Fiz. in press.

[14] M. Sorge et al., *Nucl. Phys.* **A498** (1989) 567 and papers submitted to this conference.

[15] V.N. Gribov, Proc. of the VIII LIYF Winter School of Physics, Leningrad, 1973, Vol.II, p. 5.

[16] J. Koplik and A.H. Mueller, *Phys. Rev.* **D12** (1975) 3638.

[17] J.D. Bjorken, Proc. of the Summer Inst. on Theor. Particle Physics in Hamburg, 1975, Springer-Verlag, Berlin 1976, p. 93.

[18] S. Mandelstam, *Nuov. Cim.* **30** (1963) 1113, 1127, 1148.

[19] O.V. Kancheli, *JETP Lett.* **18** (1073) 274.

[20] A.B. Kaidalov, *Physics Reports* **50** (1979) 157.

[21] J. Formanek, *Nucl. Phys.* **B12** (1969) 59.

[22] W. Czyz and L.C. Maximon, *Ann. Phys.* **52** (1969) 59.

[23] I.V. Andreev and A.V. Chernov, *Yad. Fiz.* **28** (1978) 477.

[24] A.S. Pak, A.V. Tarasov and V.V. Uzhinsky and Ch. Tseren. *Yad. Fiz.* **30** (1979) 102;
A.S. Pak, V.V. Uzhinsky and Ch. Tseren, *Yad. Fiz.* **30** (1979) 343.

[25] K.G. Boreskov and A.B. Kaidalov, *Yad. Fiz.* **48** (1988) 575.

[26] K.G. Boreskov and A.B. Kaidalov, *Acta Phys. Polonica* **B20** (1989) 397.

[27] V. Abramovsky, V.N. Gribov and O..V. Kancheli, *Yad. Fiz.* **18** (1973) 595.

[28] R. Blankenbecler et al., *Phys. Lett.* **107B** (1981) 106.

[29] C. Pajares and A.V. Ramallo, *Phys. Rev.* **D31** (1985) 2800.

[30] A. Capella and A.B. Kaidalov, *Nucl. Phys.* **B111** (1976) 477.

[31] A. Capella, Proc. of the Conference Quark matter'90, Menton.

[32] A. Capella et al., *Z. Phys.* **C3** (1980) 329;
A. Capella and J. Tran Thanh Van, *Phys. Lett.* **114B** (1982) 450.

[33] A.B. Kaidalov, *Phys. Lett.* **116B** (1982) 459;
A.B. Kaidalov and K.A. Ter-Martirosyan, *Phys. Lett.* **117B** (1982) 247; . *Yad. Fiz.* **39** (1984) 1545; **40** (1984) 211.

[34] G. 't Hooft, *Nucl. Phys.* **B72** (1974) 461.

[35] G. Veneziano, *Phys. Lett.* **52B** (1974) 220; *Nucl. Phys.* **B117** (1976) 519.

[36] L.D. Landau and I.Ya. Pomeranchuk, *Dokl, Acad. of Sci.* **92** (1953) 535; 735.

[37] E.L. Feinberg, *JETP* **50** (1966) 202.

[38] N.N. Nikolaev and V.R. Zoller, *Nucl. Phys.* **B147** (1979) 336.

[39] K.G. Boreskov et al., *Yad. Fiz.* in press.

[40] M.G. Ryskin, *Phys. Lett.* **B209** (1988) 529.

[41] A. Capella et al., preprint LPTHE Orsay 90/02 (1990).

[42] J. Varela, Proc. of the Conference Quark Matter'90, Menton.

[43] J.D. Bjorken, *Phys. Rev.* **D27** (1983) 140.